

Thermo-Fluid Dynamics of Flue Gas in Heat Accumulation Stoves: Study Cases

P. Scotton^{1,*}, D. Rossi^{1,**}, M. Barberi^{2,***}, S. De Toni^{2,***}

¹University of Padova, Department of Geosciences, Gradenigo street 6, 35131 Padova Italy

²Barberi SRL, Via Catoni 4, 38123 Trento Italy

^{1,*}paolo.scotton@unipd.it, ^{1,**}danielerossi74@gmail.com, ^{2,***}info@barberistufe.com

Abstract: The research aims to clarify some aspects of the thermo-fluid dynamics of woody biomass flue gas, within the refractory twisted conduit inside the heat accumulation stoves (ceramic-refractory stoves). The high temperature flue gas flows in the twisted conduit, releasing heat along its path to the refractory. The heat stored in the refractory is then released to the environment mainly as radiant component. The physical phenomena that occur in an accumulation stove, once provided the activation energy in the combustion chamber, continue initially increasing temperature and velocity of flue gases and then decreasing the two variables until the end of reaction. The decreasing temperatures of flue gases, flowing from combustion chamber in the twisted conduit, tends to cause the transition of the flow regime from laminar to turbulent conditions [4] [6]. This paper exposes also some analysis about the heat transport and exchange processes inside the flue gases and between them and the refractory. The numerical results, obtained with COMSOL[®] Non Isothermal Flow (k- ϵ turbulent model), have been compared with laboratory measures. In order to best represent the real cases, the models were implemented with unsteady boundary conditions and then progressively adding all the terms that can have influence on the fields of velocity and temperature [7].

Keywords: Non-Isothermal flow, turbulent flow, heat transfer, dynamics of flue gases.

1. Introduction

The research regards a particular kind of heat accumulation stoves made of ceramic and refractory. They are a traditional heating appliance of the European Alpine regions, the history of which began in the fifteenth century. They consist of a combustion chamber, where woody material is burned, followed by a twisted conduit where the high temperature products of combustion flow, transferring heat to the refractory.

Due to the heat transfer along the pipe the kinematic viscosity of the flue gas decreases

and the density increases, the Reynolds number increases causing transition from laminar to turbulent motion. Moreover the continuous changes of direction imposed by the curves, cause local contractions and expansions of the flux and, consequently, energy losses which are difficult to evaluate. The stored heat is released slowly to the environment in the form of radiant heat from the ceramic tiles of the external surface. The way the heat transfer happens depends mainly on gas flow conditions (laminar or turbulent) and on conduit physical properties (roughness of the internal surface of the conduit), as well as on the thermodynamic properties of the refractory material, its mass and its geometric arrangement.



Figure 1: Left: historical “Sfruz” heat accumulation stove, located in the Buonconsiglio Castle in Trento, Italy. Right: view of a project design of a modern stove, where combustion chamber and twisted conduit are visible.

The description of these phenomena is the goal of the present research, in order to provide increased awareness in the design process of these technological elements, which is strongly affected by the uncertainties described above. We expect to obtain important outcomes also in terms of energy saving and pollution control, giving criteria for the optimization of combustion processes and for the limitation of fine particles production. Working on that direction some physical models have been realized, by the laboratory of the Barberi Ltd [5], on which several measures of temperature, pressure and velocity, both inside the gases

and on the outer surface of the conduit have been taken.

In the present paper we show the numerical results obtained reproducing three different physical models. In the first model a straight steel pipe has been analyzed in order to define the capability of the used software to reproduce a simple, non-isothermal, steady state case. In the two following cases the refractory material used in the real heat accumulation stoves has been used, the first with the same geometry described before, the second with some curves before the entrance into the chimney. All the numerical applications have been performed on the basis of the previous experience reported also in [4] [6].

2. Analysis of the steel pipe

In this case a straight steel pipe has been used in order to try to reproduce a simple physical setup both in terms of geometry and in terms of knowledge of physical properties of the material.

2.1 Physical model

In this case hot air was introduced into the pipe (Figure 2) using a GPL heater located at the beginning of the pipe. The motion of the air inside the pipe was generated by an extractor fan placed at the end.

The pipe, 22 meters long, has been realized with modular elements having the nominal diameter of 160 mm and a thickness of 0.2 mm almost everywhere. Two elements of black steel, of thickness equal to 2 mm, have been used where the upstream and the downstream pressure measurement were taken (Table 1). From the pressure measurements it was possible to obtain the dissipative properties of the flux. The temperature measurements were realized in four sections with three thermocouples in each section. The thermocouples were placed one at the top, one at the side and one at the bottom on the external surface of the pipe.



Figure 2: the scheme of the physical model used in the experiment for non-isothermal flow with air: at the right the heat generator; the sections of temperature measurement; at the left, the extractor fan (Barberi Ltd).

The mass discharge measured by a diaphragm located at the end of the pipe, was equal to 0.0222 kg/s, where the value of the air density was 1.0574 kg/m³. At the same section the mean velocity was equal to 1.046 m/s and the temperature was 52.7°.

Figure 3 shows the three temperature measured in the four cross sections. It can be seen that after about thirty minutes from the beginning of experiment, the motion can be considered thermodynamically stationary.

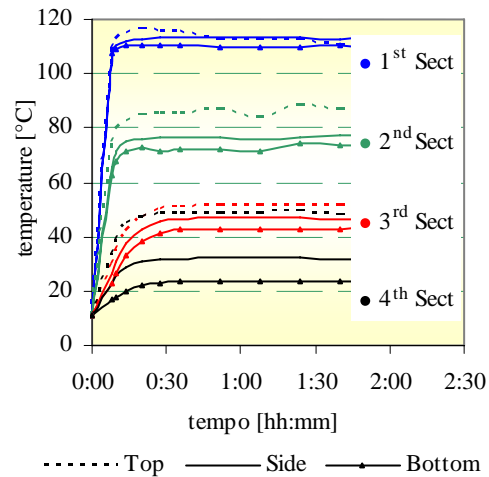


Figure 3: temperatures measured at the thermocouples in the four cross sections of the steel pipe.

	stainless steel	black steel
Thickness [mm]	0.2	2.0
emissivity [-]	0.1	0.95
conductivity [W/mK]	17	50

Table 1: thermotechnical characteristics of the different parts of the steel pipe.

2.2 Numerical model

The approach to this case study has followed a path characterized by successive steps both physical and numerical, in order to acquire sensitivity on both aspects of the problem. The 2D axial symmetry simulations (Figure 4) have the following boundary conditions:

- 1st simulation: for the convective cooling boundary condition has been used a constant value, while for the radiation from the surface to the ambient boundary condition the emissivity typical of stainless steel, also for the black steel elements, has been used;
- 2nd simulation: the constant value of convective coefficient has been replaced

with the coefficient resulting from the Nusselt equation for horizontal cylinder (Eq. 01), proposed by Churchill & Chu. The range of validity is $1 \cdot 10^{-5} \leq Ra \leq 1 \cdot 10^{12}$.

$$h = \frac{\overline{Nu} \cdot k}{L_c} \quad \text{Eq. 01}$$

were

$$\overline{Nu} = \left\{ 0.6 + \frac{0.387 \cdot Ra^{\frac{1}{6}}}{\left[1 + \left(\frac{0.559}{Pr} \right)^{\frac{9}{16}} \right]^{\frac{8}{27}}} \right\}^2 \quad \text{Eq. 02}$$

3rd simulation: the two black steel pipe elements have been represented with different properties from the stainless part of the conduit (Table 1). To verify the influence of the mesh, four simulations increasing its discretization have been made.

Beside the two-dimensional axial symmetry simulations, a 3D analysis of the first nine meters of conduit has been made, where the volume forces were considered. The buoyancy forces produce a flue gases temperature stratification with higher values in the upper part of the section. For representing the volume forces the Boussinesq approximation has been used:

$$F = \rho_r \cdot g \cdot \beta \cdot (T - T_r) \quad \text{Eq. 03}$$

where $\beta = \frac{1}{T_r}$ is the thermal expansion coefficient. In order to reduce the degrees of freedom (D.O.F.) of the linear system, only a half of the total 3D domain has been considered, obtained by a vertical symmetry plane passing through the horizontal axis of the conduit [8].

2.2.1 Mesh and Solver

The non-isothermal motion in a straight pipe has been studied considering increasing discretizations of the mesh (Figure 6). The performance of the different meshes was analyzed by solving the simplified axisymmetric problem.

First of all the thickness of the first layer of cells adjacent to the wall (h_{FL} and h_{BC} respectively the height of the first layer of the



Figure 4: the axial-symmetry domain (in red) and the 3D domain used in the numerical simulations of the steel pipe problem. Only the first part of the pipe is represented.

boundary layer and the height of the first layer of triangular cells, Table 2) has been estimated through the equation:

$$h \leq 2 \cdot \frac{11.06 \cdot \nu}{u_r} \quad \text{Eq. 04}$$

In the present case $h \leq 5.5$ mm. Known the thickness of the first layer four meshes have been constructed with the characteristics summarized in Table 2.

In Figure 5, the blue line, the thickness limit from Equation 04, is always larger than the cells height at the wall for all meshes.

	Boundary Layer [mm]	Free Triangular [mm]	D.O.F. 10^6
M1	No	$h_{BC} \leq 5.5$	0.245
M2	$h_{FL} \cong 1.0$	$h_{BC} \cong 11.0$	0.201
M3	No	$h_{BC} \cong 1.0$	1.722
M4	$h_{FL} \cong 0.25$	$h_{BC} \cong 1.0$	1.713

Table 2: Characteristics of the meshes used in the 2D simulations of the steel straight pipe (Figure 6).

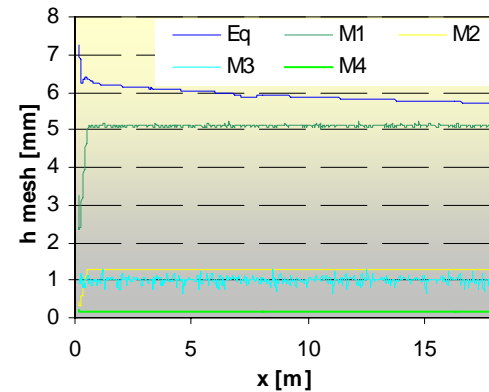


Figure 5: height of the cells adjacent to the wall along the conduit for the four cases above described.

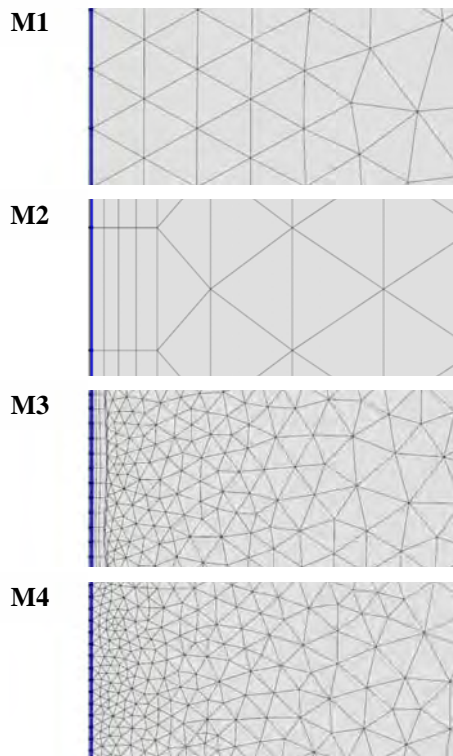


Figure 6: The meshes used in the 2D axisymmetric simulations of a straight steel pipe in non-isothermal conditions.

2.2.2 Experimental results

The results showed below regards the third simulation. The use of the first mesh (M1 in Figure 6) leads to results which differ significantly from those obtained with the use of the other three meshes, even if the rule defined by eq. 04 was respected in all cases. The 2D model is, in general, able to reproduce the decreasing trend of the temperatures along the conduit. The temperatures measured on the physical model at the first section are higher than those calculated from the numerical model, while the temperatures measured at the third section are lower.

In the first case the difference could be explained by invoking the effect of buoyancy forces, that in the first meters of the pipe are significant. As will be seen in the results of 3D simulations, neglecting the buoyancy forces is a limit for the thermo-fluid dynamics of the flue gas numerical simulations. As far as the third section is concerned, the difference between the temperatures measured on the physical model and those resulting from the numerical one, are probably due to the real characteristics of the material, that in this part of the pipe are those of the black steel (Figure 7).

The convection heat transfer between the conduit and the surrounding atmosphere were represented in the numerical simulations using the literature expressions (Eq. 01 and Eq. 02). Those expressions for a infinitely long cylinder with horizontal axis are valid for Rayleigh number ranging from $1 \cdot 10^{-5}$ to $1 \cdot 10^{12}$. As can be see in Figure 8, those limits were respected.

In Figure 9 is shown the normal conduction heat transfer on the steel wall.

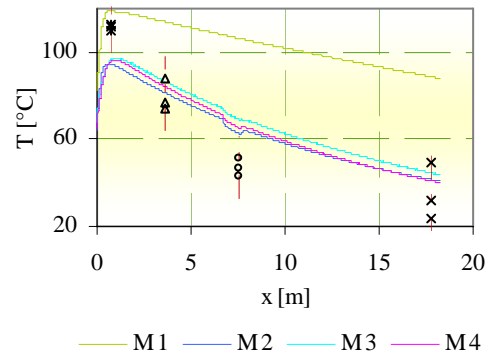


Figure 7: temperature calculated from the 2D axial symmetry model on the outer surface of the pipe; with the symbols are indicated the laboratory temperature data in the four cross sections.

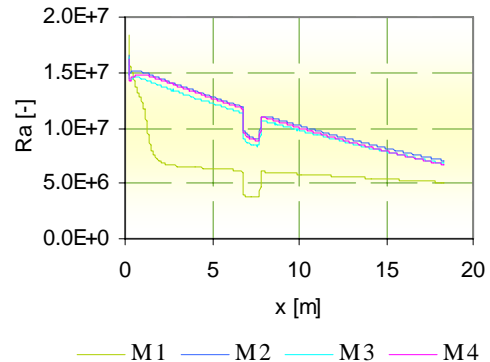


Figure 8: Rayleigh number calculated on the outer surface of the conduit fr(2D axial symmetry model).

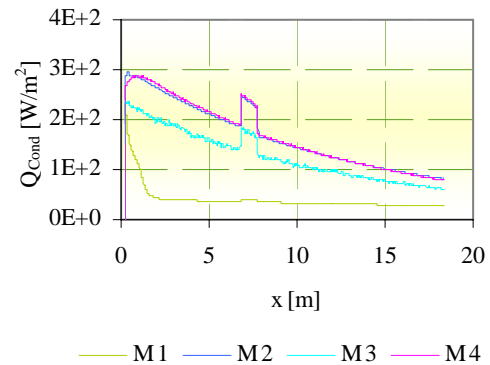


Figure 9: heat transfer by conduction in the straight steel pipe along the normal direction to the wall calculated from the 2D axial symmetry model with the four meshes.

In the 3D model, described on § 2.2, the buoyancy forces have been also considered. It was possible to highlight the temperature differences at different positions in the cross section (upper, lateral and lower point) along the pipeline (Figure 10).

The representation of the temperature trend in the upper and lateral point of the cross section is significantly improved by taking into account the buoyancy forces and changing from the two-dimensional model to the three-dimensional one (compare Figure 7 with the Figure 10). The description of the temperature trend in the lower part of the pipe is, however, not well predicted from the numerical model. From the laboratory measurements, can be deduced that the convective effect on the temperature distribution is not so significant in the first cross-section as it seems to be from the numerical simulation results (Figure 10).

Even in this simulation remain minor but still significant differences between the temperatures measured in the third section of thermocouples and the numerical results.

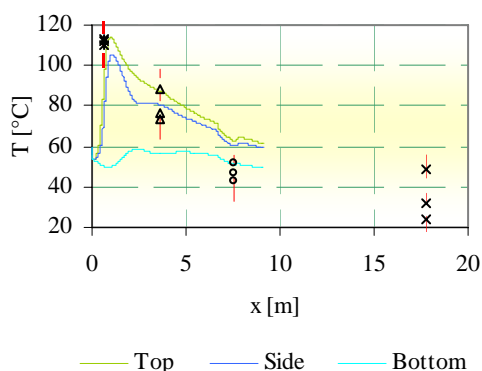


Figure 10: longitudinal temperature trend along the outer surface of the conduit in the three measurement positions: upper, lateral and lower point. The continuous line shows the numerical results; the symbols represent the laboratory temperature measures.

3 Analysis of the refractory pipes

For a simplified analysis of the heat accumulation stoves behaviour, two physical models, realized with blocks of refractory material (normally used for the construction of the stoves) have been built.

	refractory	calcespan
density [kg/m ³]	2550	600
heat cap. [J/kgK]	859	1000
conduc. [W/mK]	3.16	0.15
emiss. [-]	0.95	0.70

Table 3: Thermotechnical characteristics of materials.

3.1 Physical Models

The first physical model (*Conf. A*), is composed by the combustion chamber, 0.89 m × 0.81 m × 0.70 m, and a straight refractory conduit with total length of 6.0 m and nominal diameter of 180.0 mm (Figure 11 - A). The measures of temperature inside the flue gas are taken at the middle point of ten sections of the pipe (Gf_n). The temperatures at the outer surface are taken at 7 positions as indicated in Figure 11 - A (Te_n).

The second physical model (*Conf. B*) consists of a combustion chamber, 1.05 m × 0.61 m × 0.68 m. In this case, the refractory conduit performs four curves of 90.0 degrees. The first vertical section of the conduit is 0.6 m long, the horizontal part is 3.1 m and the second vertical section is 0.5 m long. Nine are the measure points of flue gas temperature and seven are the cross-sections where the temperature was measured on the outer surface of the conduit (Figure 11 - B).

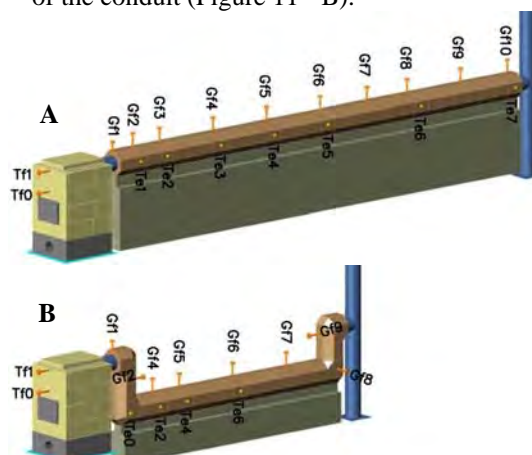


Figure 11: at the top the *Conf. A* and at the bottom the *Conf. B*, built for the simplified analysis of the behavior of a heat accumulation stove (Barberi Ltd). Gf3, Te1, Te3, Te5, Te7 are located in the non-visible part of the conduct.

The refractory conduit lies on a continuous support made of calcespan (Table 3). The combustion chambers were connected to the refractory conduit by means of a black steel pipe (Table 1). The air supply, necessary for the combustion reactions, occurred by natural draught and could be controlled by a valve (Barberi Ltd) [5].

The physical phenomena that occur in an accumulation stove, once provided the activation energy in the combustion chamber, continue initially increasing temperature and velocity of flue gases and then decreasing the two variables until the end of reaction. This causes a continuous variation in the motion

conditions at the inlet of refractory conduit. In addition, due to the heat transfer along the pipe, the gas kinematic viscosity decreases whereas the density increases, causing an increase of the Reynolds number. The variability in time of some parameters of the phenomenon can be appreciated from Table 4.

Verified that the minimum Reynolds number was greater than 4000 (for both the configurations), it was decided to use the k-ε turbulent model [3].

During the first laboratory simulation (*Conf. A*), after 150 minutes the air supply was closed with consequent reduction to zero of flue gases velocity (acting an operation which is normal in the management of the heat accumulation stoves), while in the second one (*Conf. B*) the air supply has been kept natural until the end.

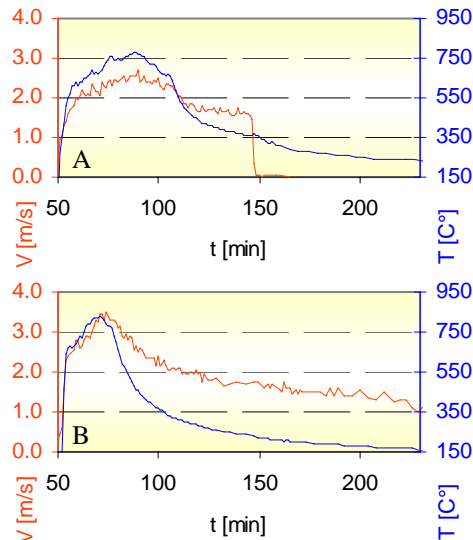


Figure 12: measured temperature and calculated velocity at the inlet of refractory conduit: above for stove A, below for stove B.

3.2 Numerical models

The simulations were carried out on the part of experimental apparatus that goes from the first part of steel conduit, necessary for connecting the heater to the refractory conduit, to the control section located in the chimney, 2.7 m above the floor.

In order to reduce the degrees of freedom (D.O.F.) of the linear system, only a half of the total 3D domain has been considered, obtained by a vertical symmetry plane passing through the axis of the conduit.

The boundary conditions for the unsteady problems with the refractory conduits are the pressure at the final section and mass discharge (calculated from laboratory data using the literature equations reported in the

prEN 15544 [9], Figure 12 and for *Conf. B* Table 4) and temperature (Gf1, Figure 11) at the initial section. In these numerical models the buoyancy forces have been represented from:

$$F = -(\rho - \rho_R) \cdot g \quad \text{Eq. 05}$$

with $dP/dz = 0$ [8].

t [min]	T _{Gf2} [°C]	ρ [kg/m ³]	V [m/s]	Re	h _{FL} [mm]
50	15.4	1.184	0.30	4067	13.9
52	150.2	0.807	0.61	4111	13.8
54	642.3	0.373	2.29	4156	13.6
71	826.7	0.311	3.44	4786	12.1
74	792.4	0.321	3.48	5061	11.5
85	536.2	0.422	2.79	6154	9.7
90	457.7	0.467	2.49	6482	9.3
94	413.7	0.497	2.36	6811	8.9
102	356.4	0.543	2.21	7390	8.3
125	269.1	0.630	1.79	7314	8.4
161	206.9	0.712	1.52	8159	7.6
293	127.9	0.852	0.98	7266	8.4

Table 4: temperatures surveyed at the Gf2 thermocouple (*Conf. B*, Figure 11/B), calculated density [9], velocity and Reynolds number of flue gas and, in the last column, the thickness required for the first cells of boundary layer.

3.2.1 Mesh and Solver

For both models, verified that the Reynolds number was greater than 4000, it was decided to use the k-ε model [3]. The characteristics of the meshes are shown in Table 5.

	<i>Configuration A</i>	<i>Configuration B</i>
h _{FL}	3.6 [mm]	2.0 [mm]
h _{BC}	29.0 [mm]	32.0 [mm]
N° El.	139.1·10 ³	481.4·10 ³
D.O.F.	175.5·10 ³	525.7·10 ³

Table 5: thickness of the first layer of boundary layer h_{FL}; minimum height of tetrahedral cells h_{BC}; total number of mesh elements N° El.; degrees of freedom of the system for the two configurations of heat accumulation stove.

3.2.2 Experimental results

For the sake of brevity and considering that the main results are similar in the two configurations, in the following the behavior of *Conf. A* is described. In Figures 13 the temperature values measured and calculated in three cross-sections are compared. In the first section, the temperature of the flue gas

measured in the middle of the conduit and calculated are in good agreement (Gf3), especially after the instant of the maximum temperature (Te2). In the other two sections the behavior tends to be the opposite. The closure of the combustion air after 150 min. produces numerical results quite different from the measured ones.

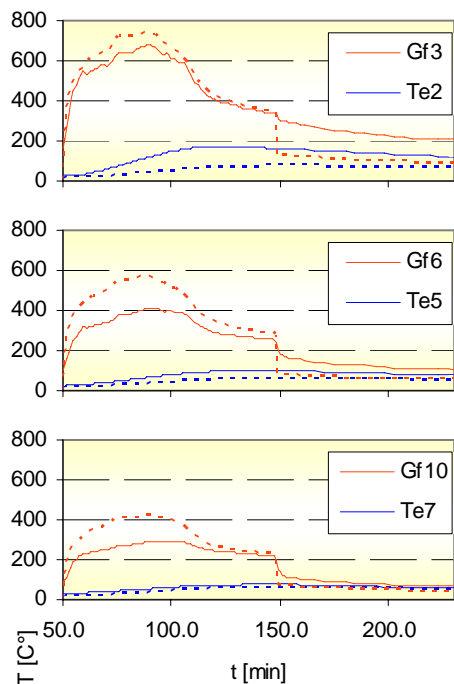


Figure 13: Configuration A, **Figure 11.** Temperatures measured on physical model (solid line) and calculated (dotted line) at three cross-sections.

4. Some final considerations

The software shows some significant differences from the laboratory data. We think that there are three main reason for the differences between numerical solutions and experimental data, and we are investigating on it. The first one is the reliability of the experimental measurements. The very challenging experimental conditions (very high temperatures, very low pressures) induce to accept high errors of the order of 20%. The second one is of numerical type: the choice of the mesh influences, in an important way, the numerical solution (Figure 6 and Figure 7). In particular, near a wall, the choice of the mesh could influence, importantly, the heat transfer through the wall. Some calculations based on the numerical results of the liminar coefficients have produced values that seem to be three or

four times lower than the physical ones. The last one is the capability to take into account all the physical phenomena which are present in the experiments. In the present simulations, for instance, the radiation between different elements of the inner surface of the conduct is not considered. Finally, we think that an important reason for the disagreement between numerical and experimental data could be the radiation absorption and emission phenomena of particle fraction of the flue gas still involved in the combustion process inside the refractory conduct [10].

The research is currently continuing, inside of the field where both the software and the spermental data may be considered reliable, in the direction of understanding of the global role of the radiation phenomena of particle fraction of the flue gas.

5. References

1. Torii S., Laminarization of strongly heated gas flows in a circular tube, *JSME International Journal*, **Vol. 33**, page 538–547 (1990).
2. Nagano J., A new low-Reynolds-Number One-Equation Model of Turbulence, *Flow, Turbulence and Combustion*, **Vol. 63**, page 135 – 151 (1999).
3. Garde R. J., *Turbulent Flow*. New Age International, (2010).
4. Scotton P., Rossi D., *Studio della dinamica del moto dei fumi nelle stufe ad accumulo – Relazione 1 anno*, (2011), prot. n. 442 (2010), department of geosciences, Univ. of Padova;
5. Barberi Ltd., 2010, personal comunication
6. Scotton P., Rossi D., 2011, Study of Gas Dynamics in the Heat-accumulation Stoves, Comsol Conference 2011 Stuttgart Proceedings, ISBN 9780983968801;
7. Scotton P., Rossi D., *Studio della dinamica del moto dei fumi nelle stufe ad accumulo – Relazione 2 anno*, (2012), prot. n. 442 (2010), department of geosciences, Univ. of Padova;
8. Comsol 4.2a manuals;
9. prEN 15544, *One off Kachelgrundöfen Putzgrundöfen (tiled mortared stoves) - Calculation method*.
10. Modest F. M., *Radiative Heat Transfer*, Academic Press, (2003).

6. Acknowledgements

The research has been financed by the Trentino (Italy) Provincial law n. 6, 1999, call 2008 - project: “La stufa ad accumulo-Innovazione nella tradizione” of the Barberi Ltd.